International Journal for Housing Science and Its Applications
Publish August 6, 2025. Volume 46, Issue 3 Pages 5904-5916

https://doi.org/10.70517/ijhsa463508

High-performance computing-based simulation to analyze the impact of biomechanical characteristics on teaching effectiveness in sports

Rui Zhang[1] and Zhe Shao[2,*]
[1] College of Sciences, North China University of Technology, Beijing, 100144, China
[2] Sports-Department, Beijing Technology and Business University, Beijing, 100048, China
Corresponding authors: (brackzr@ncut.edu.cn).

Abstract Biomechanical characteristics in sports have an important impact on teaching effect. This paper analyzes the changes of biomechanical parameters of athletes under different fatigue states through high-performance computing simulation to provide scientific basis for improving physical education and preventing sports injuries. In this study, a human musculoskeletal model was established by Anybody biomechanical simulation software, and 30 male athletes were selected as subjects, divided into 15 in the experimental group (FAI group) and 15 in the control group, and the biomechanical characteristics of lower limb joints were tested in different fatigue states (no fatigue, moderate fatigue and severe fatigue). The results of the study showed that the knee and hip flexion angles decreased significantly in the fatigue state, and the knee flexion angle at the initial touchdown moment decreased from 20.75±9.72° in the no-fatigue state to 16.94±10.24° in the severe fatigue state, and the peak knee extension moment decreased from 2.76±0.15N-m/kg in the no-fatigue state to 2.12±0.15N-m/kg in the moderate fatigue state, the vertical stiffness decreased from 58.73±14.34KN/m in the no-fatigue state to 46.47±10.45KN/m in the severe fatigue state, and there was no significant difference in the ground reaction force parameters before and after fatigue. The conclusion of the study shows that the biomechanical characteristics of the lower limbs in the state of sports fatigue change significantly, and this change may be a reflection of the human body's own protective mechanism, and by reasonably adjusting the training intensity and fatigue management can optimize the effect of physical education and reduce the risk of sports injuries.

Index Terms high performance computing, biomechanical characteristics, physical education, fatigue state, sports simulation, musculoskeletal modeling

I. Introduction

In today's physical education teaching, scientific teaching methods can not only help students master sports skills faster, but also reduce the occurrence of sports injuries and increase students' interest and motivation in sports [1]. Nowadays, scientific physical education teaching has entered the data-driven stage, which provides support for the realization of scientific physical education teaching. In most sports colleges and universities, the teaching mode of “teacher demonstration-student imitation-repeat practice” is still used in all sports programs, ignoring the individual differences of students, which leads to the poor effect of students' sports training, and even causes transient and persistent athletic injuries, and almost every year, there are cases of students' injuries due to improper training [2]-[5]. The reason for this is that the relationship between the effectiveness of physical education and biomechanical characteristics has not been explained.

In terms of human movement, biomechanics can assist in the understanding of the body's movement patterns, thus reducing sports injuries, improving sports performance, etc [6]. Biomechanics is a human study of the structure of the body and the laws of motion, which involves a number of disciplines such as mechanics, physiology and anatomy. The study of sports biomechanics can be divided into two aspects: static and dynamic. Static biomechanical analysis of movement is mainly to analyze the structural and functional characteristics of various parts of the human body by measuring and calculating the mechanical parameters of the human body, such as weight, moment, and pressure, etc., in a static state [7], [8]. For example, the analysis of human contours and musculature provides insights into the shape and size variability between individuals, thus providing fundamental data for customizing sports equipment or medical devices [9]. Dynamic biomechanical analysis of sports, on the other hand, mainly focuses on the biomechanical state of the human body in the state of movement, and this analysis method can reflect the laws of movement and kinematic characteristics of the human body in the process of movement through the calculation and measurement of various coefficients in movement, such as the speed, acceleration and energy of movement [10], [11]. For example, in track and field competitions, by analyzing the pace of competitors, their step frequency and stride length can be accurately calculated within a cycle period, so as to better understand and optimize the rhythm of the movement [12]. However, both static and dynamic studies have outstanding technical limitations. Tools such as optical capture systems that capture motion data during movement states are weak in capturing subtle motion changes. Data analysis between students' physiological change data and interaction data on the ground or teaching aids, and exercise biomechanics data are independent of each other, cross-latitude data analysis is missing, and biomechanics research models ignore individual student differences in educational settings [13]-[16]. The high-performance computing simulation analysis method, on the other hand, provides a new solution for this.

High-performance computing simulation and analysis method refers to a computing paradigm for carrying out tasks such as large-scale computing, deep learning, and data science. It mainly uses the parallel, distributed, heterogeneous and highly available characteristics of computer systems to seamlessly integrate resources such as computation, storage, network, software and human resources, so as to realize high-speed, high-efficiency and high-reliability computation and data processing [17]. High-performance computing can achieve multi-scale modeling and real-time data feedback, which is advantageous in cross-latitude data analysis, and it can analyze the mechanics of the human body structure related to movement, which highlights a greater advantage in biomechanical analysis [18]-[20].

Sports biomechanics is a discipline that studies the mechanical characteristics of human body in the process of sports and its laws, which is of great significance for sports teaching and sports injury prevention. With the development of computer technology and biomechanical testing methods, biomechanical simulation and analysis based on high-performance computing provides a new research way to study the biomechanical characteristics in sports. Biomechanical properties have both structural mechanics and material mechanics properties, and their characteristics can be reflected by load deformation and stress-strain curves. A large number of animal experiments and clinical studies have shown that experimental testing of biomechanical indexes helps to directly evaluate the quality of sports and is one of the best methods to assess the effectiveness of various sports training measures. Fatigue is an unavoidable physiological phenomenon during sports, which affects athletes' performance and increases the risk of sports injuries. Studies have shown that the biomechanical characteristics of lower limb joints change under different fatigue states, and these changes may affect the effectiveness of physical education and the safety of athletes. However, there are fewer studies on the changes of biomechanical characteristics in sports under different fatigue states and their effects on teaching effectiveness. In this study, the changes of biomechanical characteristics such as kinematic indexes, kinetic indexes, ground reaction forces and stiffness of athletes' lower limb joints were investigated by establishing human musculoskeletal models and high-performance computational simulation analysis in the three states of no-fatigue, moderate-fatigue and severe-fatigue. Anybody biomechanical simulation software was used to establish a complete musculoskeletal model of the human body, and the experimental data were collected with the Vicon 3D motion capture system and the AMTI 3D force platform, and the simulation model was verified by the complex correlation coefficients between the surface electromyographic signals and the muscle forces. Thirty male athletes were selected as subjects for the study, divided into experimental and control groups, and the qualification of subjects was determined by methods such as questionnaire screening and front drawer test. The experimental process included static collection, warm-up, maximum vertical jump test, movement practice, movement test in no fatigue state, moderate fatigue movement test and severe fatigue movement test. Through this series of experimental design and data collection, this study aims to comprehensively analyze the changes of biomechanical characteristics in sports under different fatigue states and explore the effects of these changes on the effectiveness of physical education teaching. The results of the study will provide a scientific basis for training load control, sports technology guidance and sports injury prevention in sports teaching, and will also provide an example reference for the application of high performance computing in sports research. In addition, by understanding the changing rules of biomechanical characteristics under different fatigue states, it can help physical education teachers and coaches to better design training plans and teaching programs, and improve the relevance and effectiveness of physical education teaching.

II. Research object and methodology

Biomechanical properties have both structural and material mechanical properties, which can be reflected by the load-deflection curve. The mechanical properties of materials refer to the mechanical properties of biological tissues, which have nothing to do with their geometrical shapes and can be reflected by the stress-strain curves. The results of a large number of animal experiments and clinical studies have shown that experimental testing of biomechanical indexes can help to directly evaluate the quality of sports and is one of the best ways to assess the effectiveness of various sports training measures.

II. A. Subjects and research indicators

II. A. 1) Experimental subjects

In this study, according to the unified sports screening criteria proposed by the International Sports Association, 15 male athlete subjects were selected as the experimental group, i.e., the FAI group, through the questionnaire screening combined with the front drawer test and other methods. The FAI group was matched with 15 male athletes with lower limb joint injuries as the control group according to their age, height, weight and other morphologic indicators, years of experience in sports and sports programs. The experimental site was the Laboratory of Sports Biomechanics, University of S. The study was reviewed by the Scientific Research Ethics Committee of S University.

The inclusion criteria for the FAI group were as follows:

(1) At least 1 lower extremity joint sprain, with the initial sprain occurring at least 12 months prior to the experiment, and symptoms of inflammation such as pain and swelling that interrupted physical activity for at least 2 days.

(2) Previous recurrent sprains of lower extremity joints, and/or experience of "destabilization".

(3) A score of less than 25 on the Cumberland Articular Instability Inventory (CAIT).

(4) All subjects did not engage in strenuous exercise within 1 day prior to the experiment.

Exclusion criteria for the FAI group were as follows:

(1) Previous history of surgery and fracture of the musculoskeletal structures (bones, joints, and nerves) of the lower extremities.

(2) Acute injury to the musculoskeletal structures of the lower extremities in the 30 days prior to the official experiment, affecting the normal functioning of the joint muscles and resulting in an interruption of physical activity for at least one day.

(3) Lower extremity joint sprains, and/or recurrent sprains, and/or experience of "destabilization".

(4) A positive anterior drawer test of the joints of the lower extremities.

II. A. 2) Research indicators

(1) Kinematic indicators. Landing stabilization time, arrival time of the peak ground reaction force in each direction, corresponding time of the maximum angle of knee flexion and ankle extension, instantaneous angle and maximum angle of the knee and ankle joints at different moments, and the maximum angular velocity of the knee and ankle during landing. The amount of angle change during the feedforward time = |angle at the moment of touchdown - angle at the moment 100ms before touchdown|.

The stabilization time (TTS) is defined as the moment when the foot touches the force platform at the moment of landing, and the moment when the ground reaction force in the vertical direction is equal to one's own body weight and the fluctuation of GRF is within 5% of the body weight in the following 10ms as the end point. The feed-forward phase was also defined as starting at 100ms before touchdown and ending at foot touchdown. The knee-ankle feedforward in the following section represents the amount of angular change from 100ms before knee-ankle touchdown to the moment of touchdown, respectively.

(2) Kinetic indicators. Kinetic metrics are weight-normalized peak ground reaction forces (BW%) vertically in the vertical direction GRF (VGRF), forward in the forward direction GRF (AGRF) and backward in the backward direction GRF (PGRF), inward in the inward direction GRF (MGRF), and outward in the outward direction GRF (LGRF), and the loading rate vertically (inward and outward refers to the distance of a structure of the human body from the body's relative proximity to the median sagittal plane). Where the peak ground reaction force in each direction is normalized, i.e., GRF peak relative value = GRF peak/mg. Load rate (LR) in body weight per second (BW/s) is given by the formula Load rate in the vertical direction = peak ground reaction force in the vertical direction/time to reach the peak.

(3) Surface E&M metrics. Root-mean-square amplitude (RMS) is an indicator of changes in the magnitude of the EMG signal amplitude, which is thought to be related to motor unit recruitment and synchronization of excitatory rhythms, and is positively correlated with the degree of muscle fiber recruitment. It is calculated as:

$$RMS = \sqrt{\frac{1}{N}\int_{i=1}^{N} EMG(i)^2\, dt} \tag{1}$$

The integral EMG value (sEMG) refers to the total number of motor unit discharges in a muscle involved in an activity over a period of time. sEMG values reflect the number of muscle units participating in a movement at a constant time, and they have been used to assess neuromuscular responses in a range of activities. It is calculated as:

$$sEMG = \int_{N_2}^{N_1} |X(t)| dt \tag{2}$$

II. B.Research methodology

II. B. 1) Main equipment for the experiment

The Vicon 3D motion capture system, with a frequency of 220Hz, mainly includes a host system for data collection and analysis, infrared reflective Mark points, and a motion capture camera, all of which are manufactured by OM.

(1) Host system. Mainly Vicon nexus, in this software interface real-time, dynamic simulation and output of the athlete's three-dimensional spatial trajectory of the data, and at a later stage to be able to modify and supplement the error and missing Mark points, to store the relevant kinematic data in the form of C3D data.

(2) Infrared reflective Mark points and motion capture camera. Ten 5-megapixel Vicon-T40s motion capture cameras (0-3000 frames/sec) are symmetrically distributed in the experimental site with the 3D force platform on the ground as the center, which can track and capture the infrared reflective Mark points marked on the bony anatomical structures of the human body, and the output can be dynamically recorded on the Vicon 3D motion capture system during the whole HSPL process, which is capable of recording the 3D trajectory of human movement. 3D motion trajectory of human movement [21].

AMTI three-dimensional force platform, frequency of 1500 Hz. force platform is widely used in the field of human biomechanics research, can real-time, dynamic measurement of the human body static standing or impact on the ground, the human body by the ground impact force. In this experiment, the AMTI 3D force table software was used to analyze the ground force on the human body during the HSPL process, i.e., the ground reaction force. Including vertical, left-right and front-back directions, the human musculoskeletal model was established based on the ground reaction force, and the reverse dynamics was analyzed.

II. B. 2) Experimental data collection

In order to better obtain relevant sports experimental data, this paper proceeds through the following steps, namely:

(1) Signing the informed consent form and filling in personal information (height, weight, age, specialized sports level, injury history, etc.), changing the tight shorts and flat shoes uniformly equipped in the laboratory.

(2) After the static collection, subjects completed a 6-10min brisk walking warm-up on the running platform at a speed of 5km/h. Appropriate stretching was performed at the end of the session to avoid sports injuries due to insufficient preparatory activities during the subsequent experiments.

(3) Maximum vertical jump test. After the warm-up activity, the maximum absolute height of the subject's in situ vertical jump was measured. Subjects were asked to perform three maximal effort vertical jumps on the force platform, and the best of the three jumps was taken as the subject's maximal vertical jump height after calculating the absolute height of the three jumps.

(4) After the preparatory activities, the experimenters informed the subjects about the whole experimental procedure, and the subjects completed 3~5 exercises under the guidance of the experimenters to familiarize themselves with the experimental movements on the field, and adjusted the position of the subjects to make sure that the final landing point was in the middle of the two force platforms with both feet stepping on the two force platforms. At the same time, the whole movement is completed without discomfort and can play full force, to be confirmed by the position of the subject and adapt to the field after the start of the formal experiment.

(5) Movement test under non-fatigue (NF) condition. Subjects in the non-fatigue state according to the requirements to complete five 50cm height and four 50cm height of the deep jump movement test.

(6) Moderate fatigue (MF) movement test. After the subjects reached moderate fatigue in the fatigue program, they completed the corresponding movement test.

(7) Severe fatigue (SF) movement test. Subjects continue to execute the fatigue program on the basis of moderate fatigue, and complete the corresponding movement test when they reach the state of severe fatigue.

(8) Relaxation and stretching, supplementation, and end of experiment.

Based on the above steps, the experimental flow was obtained as shown in Figure 1.

II. B. 3) Simulation Modeling

(1) Anybody Biomechanical Simulation Software

Anybody is a human body modeling and simulation software for biomedical and ergonomic fields. The software can provide all the kinematics, dynamics and biomechanics related parameters of the human skeletal-muscular system model in contact with the external environment, and calculate the skeletal-muscular activity, joint force and other information related to the working characteristics of the human body. It has been widely validated and recognized in the fields of basic medicine, clinical applications, industrial design, robot design and rehabilitation medicine [22].

Currently, human biomechanics simulation software includes Anybody and SD/Fast, etc. Anybody has its own advantages in the following aspects compared with other software:

Complete human musculoskeletal model. The human physiology model is very complex, and it can't be simulated at the beginning of each analysis. The database of this software has already defined the complete human body model, including bones, muscles, joints and ligaments. Moreover, it is possible to modify the position, body parameters and rotational inertia parameters of the model based on the original model.

Good compatibility and data conversion Anybody has a variety of modeling methods, first, you can build your own model in the software, but in the establishment of more complex models, the function is a little single. Second, through other 3D software into STL format, can be imported into the software. In addition, Anybody software can export the human bone and muscle model data into ANSYS and ADAMS software can recognize the data, greatly improving the user experience.

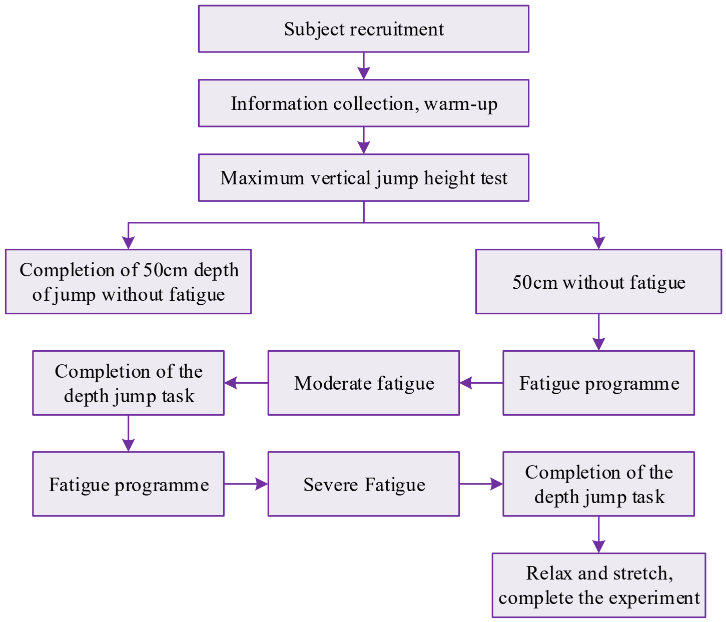

Figure 1: Experimental procedure

Anybody's unique programming language is AnyScript, similar to C and Java, which can be queried and used in the software database at any time, and the interface is simple and intuitive, which makes it easier for beginners to get started. Anybody can directly import gait data (C3D format), which makes data analysis and processing more convenient. Anybody can import gait data (C3D format) directly, which makes data analysis and processing easier and more convenient.

Inverse dynamics modeling. Inverse dynamics is the study of how a given model achieves a particular state of motion, and then using inverse dynamics algorithms, parameters such as joint angles, joint contact forces, muscle moments, net joint moments, and muscle forces can be calculated precisely.

Anybody software can be used in many fields such as ergonomics, biomedical engineering research, rehabilitation medicine, sports science and so on.

(2) Simulation Modeling

Anybody model system is currently the only complete musculoskeletal model of biomechanical analysis software, the core principle of its operation is the inverse dynamics analysis.Anybody software can simulate a variety of human movement state, and in a particular state to analyze its muscles, bones, joints and the elasticity of the tendon and other characteristics, can provide a platform for biomedical engineering research [23].

Anybody model can be generated by the corresponding musculoskeletal models for different sizes of the human body, the system's built-in scaling criterion function or Ran defined scaling criterion function to scale the default model in the system, can be better to establish more suitable for the experimenter's human body parameter-based musculoskeletal model. Due to the large number of spinal muscles, the number of muscles is larger than the degree of freedom of the musculoskeletal model, resulting in the inability to accurately analyze the muscle activity, in order to solve this problem, this experiment is used in Anybody Modeling System in the maximum/minimum model. Namely:

$$\min G\left(F^{M}\right) \tag{3}$$

$$G\left(F^{M}\right)=\max\left(A_{i}^{M}\right)=\max\left(\frac{F_{i}^{M}}{N_{i}}\right) \tag{4}$$

$$CF^{M}=R \tag{5}$$

$$F_{i}^{M}\geq 0,\, i\in\left\{1,2,\cdots,n^{M}\right\} \tag{6}$$

where F_i^M is the muscle force of the i th muscle, A_i^M is the muscle activation, i.e., the ratio of muscle force to muscle strength, N_i is the muscle strength, i.e., the maximal force supplied by the muscle at its optimal length, C is the matrix coefficient, R is the ground reaction force, and n^M is the total number of muscles. The model assumes that muscle activation is positively correlated with muscle fatigue, and maximum muscle activity is generated based on the assumption of minimum muscle fatigue.

The construction of the human torso simulation model in the Anybody model includes the head (C0) as a rigid body, the neck (C1-C7) as a rigid body, the thoracic vertebrae (T1-T12) as a rigid body, the lumbar vertebrae (L1, L2, L3, L4, and L5) as a rigid body respectively, the sacral vertebrae (S1-S3) as a rigid body, and the pelvis (P) as a rigid body, and the connection between the rigid bodies is considered as a Joints. A complete muscle model of the lumbar region was established based on the anatomy of the trunk muscles. The model was driven in two steps in the experiment, the first step first kinematics, after importing the data, the spine kinematics indexes at each time point (6ms) were calculated, such as lumbar curvature, cervical curvature, angular velocity, angular acceleration, velocity, displacement, acceleration and other kinematics indexes of each segment. In the second step of reverse kinetics, biomechanical data of each part of the human body at each time point (6ms) were calculated, such as reaction forces between each joint (compression force in the Z-axis direction, shear force in the X-axis direction, and medial-lateral force in the Y-axis direction), moments at the upper and lower ends of the spinal column, individual muscle forces, muscle activation, and muscle forces as a function of muscle length, and so on.

(3) Simulation model solution

Anybody uses inverse dynamics to solve the model for muscle forces and joint loads. The key to this method is to solve the muscle redundancy problem, i.e., the human body contains a much larger number of muscles than the number of muscles required to balance the external load, and some of the muscles are in an unconstrained state, so that a set of equations of motion can produce an infinite number of solutions [24]. Therefore, to solve the muscle redundancy problem, the musculoskeletal external load balancing equations are established in the software as follows:

$$Cf=d \tag{7}$$

where C is the coefficient matrix, f is the vector sum of muscle forces, and d is the vector of applied external loads.

From a physiological point of view, muscle redundancy tends to be systematic, and from a mathematical point of view, solving the muscle redundancy problem can be viewed as an optimization problem, i.e., minimizing the muscle and body loads, by defining the design variables as f_i^M, and the objective function and constraints as follows:

The objective function is:

$$MinG_{(f)}=G\left(f_{i}^{M}\right) \tag{8}$$

The constraints are:

$$0\leq f_{i}^{(M)}\leq N, i\in\left\{1,2,\cdots n\right\} \tag{9}$$

where G is the objective function, i.e., the system's selection strategy for muscle force, f_i^M is the muscle force of the i th muscle, and N is the limiting strength of the muscle, which is greater than ≥0 because the muscle itself can only be stretched but not compressed.

The muscle Min/Max fatigue criterion (Min/Max Strict) in Anybody software, which is the muscle force allocation follows the principle of minimum optimization for maximum activity. I.e.:

$$MinG\left(f\right)=Max\left(A_{i}^{m}\right)=Max\left(f_{i}^{M}\big/N_{i}\right) \tag{10}$$

where A_i^M is the muscle activity, f_i^M is the maximum muscle force of the i th muscle, and N_i is the stretch intensity of each muscle in the current working state.

As the number of muscles involved in balancing increases with it, the coordination between the muscles becomes better and better. When the muscles involved in the balance reach the maximum, the forces on the muscles become small relative to the external loads, and the low-loaded muscles assist the high-loaded muscles in their activities, realizing the optimal inter-muscular collaboration.Anybody software applies the inverse dynamics external load balance equations and the Min/Max Strict to realize the muscle striving solution for the musculoskeletal model.

Muscle activation reflects the degree of activity of individual muscles during exercise and is the most intuitive parameter to measure the degree of fatigue of an athlete, which is expressed by the formula:

$$A_i = \frac{F_i}{F_{MAX}} \times 100\% \tag{11}$$

$$F_{MAX} = M_\sigma \times PCSA \tag{12}$$

where A_i is the muscle activation level of the i th muscle, F_i is the muscle force of the i th muscle, F_{MAX} is the maximal muscle force of the i th muscle, M_σ is the maximal tissue stress of the muscle, and $PCSA$ is the physiological cross-sectional area of the muscle.

II. B. 4) Data processing and statistics

Raw surface EMG data were processed using Noraxon MyoResearch. Filtering (band-pass filtering, FIR at 10-500 Hz) rectification, smoothing filtering (based on the RMS algorithm, with a window value set to 60 ms), and amplitude normalization (other recorded values-MVC) were performed sequentially. The data were intercepted from the surface EMG values of subjects with a time length of 12s after the terminal muscle contraction was stabilized for 2s. Finally the data were exported to obtain the root mean square amplitude (RMS) and integral EMG values (iEMG).

The statistical analysis of the study was performed using Excel, Origin, and SPSS software. The relevant biological characteristics data were imported into Excel, the mean value was calculated for each individual for five times, and then the mean and standard deviation were calculated for each individual in different modes, and the data were imported into Origin software, and the data were represented using graphical forms. Compare the differences in the data of biological characteristics in different modes. One-way ANOVA was performed using SPSS software to arrive at the desired results, with the significance level taken as 0.05, with P<0.05 indicating a significant difference and P<0.01 a highly significant difference. This study focuses on the comparative analysis between multiple fatigue states and analyzes the changes in biomechanical characteristics of the subjects under the sport by computational simulation.

III. Experimental results and discussion

Sports biomechanics study of human movement in sports, the main task is to use mechanical methods to make the complex system mathematization, and then the human body movement phenomenon for objective and quantitative description and explanation. Its mechanical basis is classical mechanics and material mechanics, and its biological basis is the structure and function of human movement system, such as the geometric size and strength characteristics of bone, ligament, tendon, and the degree of freedom of joint movement, which also includes the mechanical characteristics of muscle under various contraction conditions, according to which biomechanical principles are established in order to evaluate the human movement technology.

III. A. Simulation model simulation verification results

The simulation results of gluteus maximus, rectus femoris, lateral femoris, biceps femoris, semitendinosus, tibialis anterior, and gastrocnemius medial and lateral head muscle simulation were verified during sports activities of athletes in a fatigue-free state. Simulation analysis was carried out based on the human kinematics model established by Anybody simulation model. In addition, the trend of surface electromechanical signals versus muscle force was quantitatively verified by the complex correlation coefficient. Figure 2 shows the curves of muscle force and surface EMG signals, where Figures 2(a)~(h) show the simulation results of gluteus maximus, rectus femoris, lateral femoris, biceps femoris, semitendinosus, tibialis anterior, and medial and lateral head of gastrocnemius, respectively. Table 1 shows the results of the analysis of the complex correlation coefficients for both.

As can be seen from the figure, the surface EMG signal curve and the muscle force simulation result curve have the same trend of change, but there are some differences. The two trends were quantitatively verified by the complex correlation coefficient, and the correlation analysis showed that the CMC of each muscle was greater than 0.8, with the CMC of the tibialis anterior and the medial head of the gastrocnemius muscle>0.91, and the muscle CMC of the gluteus maximus, biceps femoris, lateral head of the gastrocnemius muscle, rectus femoris, lateral femoris muscle, and semitendinosus muscle were all greater than 0.8. It is suggested that the lower limb muscle force simulation results during sports are highly similar to the electrophysiological data. In addition, the same human musculoskeletal model was used in moderate and severe fatigue states, and the validation results will not be repeated. In summary, the validity of the human musculoskeletal model in Anybody system in this study is proved, suggesting that the results computed by this model can be used in the next step of analysis and research.

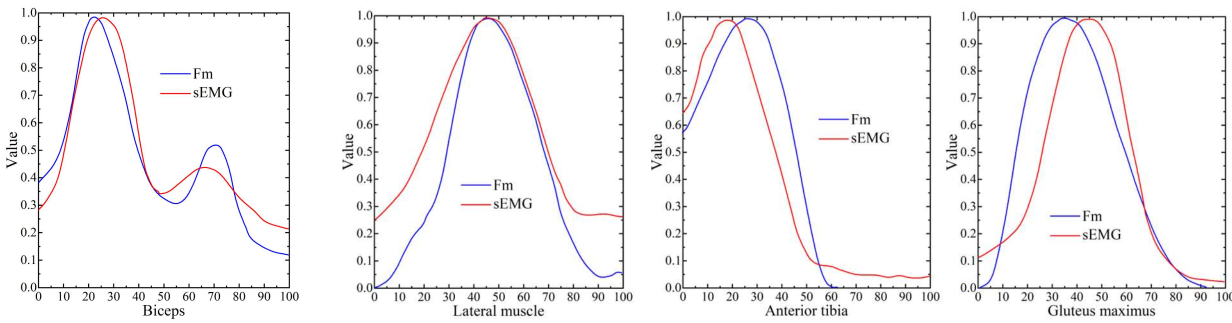

(a) Biceps (b) Lateral muscle (c) Anterior tibia (d) Gluteus maximus

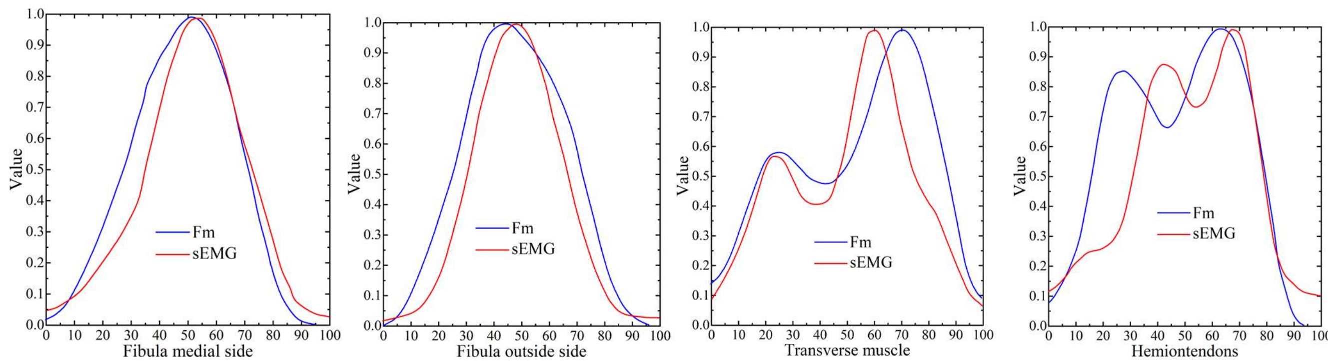

(e) Fibula medial side (f) Fibula outside side (g) Transverse muscle (h) Hemiontendons

Figure 2: Muscle Force Simulation Result Curve and sEMG Curve

Table 1: Analysis results of complex correlation coefficients

Muscle Name	Gluteus maximus	Transverse muscle	Lateral muscle	Biceps
CMC	0.895	0.833	0.821	0.842
Muscle Name	Hemiontendons	Anterior tibia	Fibula outside side	Fibula medial side
CMC	0.819	0.936	0.884	0.917

III. B. Simulation under different fatigue states

III. B. 1) Kinematic indicators of lower limb joints

(1) Hip joint angle

The data of lower limb joint kinematic indexes of the subjects in different fatigue states were counted and analyzed by one-way repeated measures of variance. Table 2 shows the hip joint angles at different fatigue levels, and # in the table indicates $P<0.05$ compared with the no-fatigue state.

One-way repeated measures ANOVA showed that there were statistically significant differences in hip flexion angles at initial ground contact ($p=0.015$) and peak vGRF moment ($p=0.015$) at different levels of fatigue ($P<0.05$). Further tests revealed that after moderate fatigue, the hip flexion angles at initial ground contact ($p=0.020$) and peak vGRF moment ($p=0.022$) were significantly smaller than in the non-fatigued phase ($P<0.05$). After severe fatigue, the hip flexion angles at initial ground contact ($p=0.030$) and peak vGRF moment ($p=0.035$) were also significantly smaller than in the non-fatigued phase ($P<0.05$). Additionally, there were no statistically significant differences in hip adduction/abduction angles and rotation angles at different levels of fatigue.

Table 2: Hip joint angles at different degrees of fatigue

Variable	NF	MF	SF
Hip joint Angle at the initial moment of contact			
Flexion/extension Angle	43.19±7.38	36.78±9.48#	40.12±10.54#
The Angle of adduction/abduction	0.52±6.14	0.67±7.52	-1.88±4.45
Internal rotation/external rotation Angle	6.34±12.05	5.83±15.14	10.46±13.32
Hip joint Angle at peak vGRF moment			
Flexion/extension Angle	45.42±8.96	38.95±9.29#	41.75±10.84#
The Angle of adduction/abduction	1.05±6.15	1.59±7.23	-1.26±4.68
Internal rotation/external rotation Angle	6.56±11.48	6.12±13.84	10.76±14.15

(2) Knee Joint AnglesTable 3 shows the knee joint angles at different levels of fatigue. There are significant differences in the knee joint flexion angles at the initial ground contact moment ($p=0.045$) and at the peak vertical ground reaction force (vGRF) moment ($p=0.008$) across different fatigue levels ($P <0.05$). Further testing revealed that following moderate fatigue, the knee joint flexion angles at the initial ground contact moment ($p=0.030$) and at the peak vGRF moment ($p=0.008$) were both significantly smaller than those in the non-fatigue phase ($P<0.05$). After severe fatigue, the knee joint flexion angles at the initial ground contact moment ($p=0.020$) and at the peak vGRF moment ($p=0.008$) were also significantly smaller than those in the non-fatigue phase ($P <0.05$). However, there were no statistical differences in the knee joint adduction/abduction angles and rotation angles at the initial ground contact moment and peak vGRF moment at different levels of fatigue ($P >0.05$).

Table 3: Knee joint angles at different degrees of fatigue

Variable	NF	MF	SF
Knee joint Angle at the initial moment of contact with the ground			
Flexion/extension Angle	20.75±9.72	17.46±8.05#	16.94±10.24#
The Angle of adduction/abduction	-2.36±6.64	-4.66±5.18	-0.93±7.21
Internal rotation/external rotation Angle	-7.11±7.89	-7.26±9.93	-9.88±14.46
The knee joint Angle at the peak vGRF moment			
Flexion/extension Angle	26.31±9.45	20.55±8.56#	21.21±10.06#
The Angle of adduction/abduction	-1.95±6.79	-4.53±5.69	-0.32±7.96
Internal rotation/external rotation Angle	-5.72±8.36	5.78±10.92	-7.99±15.14

III. B. 2) Indicators of lower extremity joint kinetics

Table 4 shows the changes of hip joint moments under different degrees of fatigue. As shown in the table, there was no significant difference in hip flexion, adduction and internal rotation moments at the moment of touchdown at different degrees of fatigue landing, and there was no significant difference in peak flexion, abduction and external rotation moments during buffering. The joint moments can reflect the trend of joint movement, and according to the hip moment parameters, it can be seen that the hip joint shows the trend of internal retraction and internal rotation during landing cushioning.

Table 4: The variation of hip joint torque (N·m/kg)

Variable	NF	MF	SF
Hip joint torque at the moment of contact			
Flexion/extension	0.16±0.09	0.06±0.15	0.08±0.15
Internal acquisition/external expansion	0.03±0.02	0.04±0.03	0.02±0.05
Internal rotation/external rotation	0.04±0.05	0.05±0.12	0.02±0.16
The peak torque of the hip joint during the buffering process			
Flexion/extension	2.85±0.72	3.06±0.45	2.62±0.48
Internal acquisition/external expansion	0.22±0.41	0.15±0.12	0.15±0.17
Internal rotation/external rotation	0.13±0.23	0.15±0.11	0.16±0.08

Table 5 shows the changes in knee joint torque under different levels of fatigue, where # indicates a significant difference compared to moderate fatigue ($P<0.05$). During the landing phase, exercise fatigue significantly affects knee joint torque, with the peak knee extension torque decreasing from 2.76±0.15 N•m/kg under no fatigue to 2.12±0.15 N•m/kg under moderate fatigue, showing a significant difference between the two states ($P<0.05$). There are no significant differences in knee joint flexion, adduction, and internal rotation torque at the moment of touchdown during landing under different fatigue levels, nor in the peak values of knee joint torque for abduction and external rotation during the landing phase. However, knee torque parameters indicate that the hip joint tends to exhibit adduction and internal rotation during the landing phase.

Table 5: The variation of knee joint torque (N·m/kg)

Variable	NF	MF	SF
Knee joint torque at the moment of contact			
Flexion/extension	0.21±0.15	0.14±.18	0.32±0.22
Internal acquisition/external expansion	0.13±0.34	0.15±0.33	0.25±0.18
Internal rotation/external rotation	0.06±0.03	0.05±0.02	0.06±.03
The peak torque of the knee joint during the buffering process			
Flexion/extension	2.76±0.15#	2.12±0.15	2.34±0.38
Internal acquisition/external expansion	0.32±0.28	0.25±.33	0.24±0.15
Internal rotation/external rotation	0.05±0.08	0.04±0.02	0.06±0.04

III. B. 3) Ground reaction forces and rigidity

Table 6 shows the data related to the ground reaction force under different fatigue states. In the table, Fzmax1 denotes the impact force (i.e., the first peak value of ground reaction force), t_Fzmax1 denotes the time to reach Fzmax1, LRmax denotes the maximum loading rate, and LRavg denotes the average loading rate. Fzmax2 represents the stirrup force (i.e., the second peak of the ground reaction force). t_Fzmax2 denotes the time to reach Fzmax2, CT denotes the time to touchdown, Fymax denotes the peak braking force in the horizontal direction, and Fymin denotes the peak propulsive force in the horizontal direction.

No significant differences were observed in ground reaction force parameters such as the first and second peak values and their arrival times, touchdown time, average and maximum load factor, and horizontal direction maximum and minimum values for the 2 moments of moderate and severe fatigue compared to the fatigue-free condition. In addition, none of the above parameters were also significantly different between the moments.

Table 6: Ground reaction forces under different fatigue states

Parameters	NF	MF	SF
Fzmax1 (BW)	1.76±0.23	1.75±0.24	1.74±0.18
t_Fzmax1 (s)	0.05±0.02	0.05±0.02	0.03±0.02
LRmax (BW/s)	97.48±16.02	98.54±20.08	100.94±20.81
LRavg (BW/s)	86.24±15.24	88.92±15.17	92.04±15.16
Fzmax2 (BW)	2.45±0.15	2.43±0.26	2.46±0.19
t_Fzmax2 (s)	0.08±0.02	0.08±0.02	0.08±0.02
CT (s)	0.23±0.03	0.24±0.02	0.24±0.01
Fymin (BW)	-0.43±0.08	-0.46±0.07	-0.47±0.08
Fymax (BW)	0.34±0.05	0.32±0.05	0.33±0.05

Table 7 shows the changes in joint stiffness and vertical stiffness under different fatigue states. Kleg in the table represents vertical stiffness, Δy represents the change in vertical displacement of the center of gravity, and Kankle, Kknee, and Khip represent the stiffness of the ankle joint, knee joint, and hip joint, respectively. # indicates a significant difference with fatigue interventions ($P<0.05$). There is a significant change in vertical stiffness across different fatigue states ($P<0.05$), and post hoc tests indicate that compared to the non-fatigue state, vertical stiffness significantly decreases in moderate and severe fatigue states ($P<0.05$). Additionally, there is a significant change in the vertical displacement of the center of gravity under fatigue conditions ($P<0.05$), with post hoc tests showing that compared to the non-fatigue state, the vertical displacement of the center of gravity significantly decreases in moderate and severe fatigue states ($P<0.05$). However, there were no significant changes observed in the joint stiffness of the ankle, knee, and hip joints, and there were no significant differences in the above measurements across different fatigue states ($P>0.05$).

Table 7: The changes of joint stiffness and vertical stiffness

Parameters	NF	MF	SF
Kleg (KN/m)	58.73±14.34	50.26±9.61#	46.47±10.45#
Δy (cm)	3.28±0.61	3.69±0.53#	3.98±0.76#
Kankle (N·m/kg/°)	0.23±0.05	0.15±0.08	0.17±0.09
Kknee (N·m/kg/°)	0.09±0.04	0.12±0.11	0.08±0.05
Kkip (N·m/kg/°)	0.76±0.52	0.78±0.54	0.72±0.47

III. C. Discussion of different fatigue states

III. C. 1) Kinematic indicators of lower limb joints

In this study, the lower extremity kinematic indexes at the moment of initial touchdown and the moment of peak vGRF were selected for analysis and investigation. By analyzing the kinematic indexes of the lower extremity at the initial touchdown moment during single-leg landing, it is possible to investigate the immediate performance pattern of the lower extremity joints in response to the ground impact force. In addition, the lower limb kinematic indexes at the moment of peak vGRF were chosen to be analyzed because it has been shown that the vertical ground reaction force tends to peak at the same time as the total ground reaction force, and that the maximum value of ACL tension after landing often occurs at the peak moment of ground reaction force. The results of the present study showed that subjects did undergo some unfavorable changes that may increase ACL loading, such as a decrease in hip and knee flexion angles, during the fatiguing post-jump landing maneuver.

The subjects in this study also showed a significant reduction in knee flexion angle after heavy fatigue close to exhaustion compared to pre-fatigue. The reason for the same result may be that the study did not induce fatigue in the flexor muscles alone, but the flexor muscles are involved in the process of sustained running. Moreover, the study considered the subjects' inability to continue exercise as the end point of fatigue induction, i.e., the subjects' leg muscles reached a fatigued state, and as mentioned above, the flexor knee muscles are more susceptible to fatigue than the extensor knee muscles, which led to the same results as in the present study.

The results of the present study showed that the subjects' hip flexion angle was significantly reduced after both moderate and severe fatigue compared to pre-fatigue. This phenomenon may be due to the fact that both the present study and the existing study used a single-leg landing task with forward jumps, and that the study used the inability to continue the knee extension maneuver as the fatigue-inducing termination criterion, at which time the knee flexors also reached a high level of fatigue.

III. C. 2) Indicators of lower extremity joint dynamics

The knee extension moment was significantly and positively correlated with the anterior tibial shear force, which in turn was closely related to the tension of the ACL. Therefore, knee extension moment can be used as an important index to respond to the magnitude of ACL loading. In this study, we found that the peak value of knee extension moment was reduced in the state of heavy fatigue, which indicated that when the body has a certain degree of fatigue, due to the adaptive and regulatory ability that the human body itself has, the kinematic characteristics of the lower limbs can be changed by changing the kinematic characteristics of the lower limbs, such as increasing the amount of change in the angle of the joints of the lower limbs, in order to increase the lower limb extensor muscle groups centrifugal contraction work distance and time to help the muscles absorb the reaction force from the ground.

At the same time, the increase of joint flexion angle and the decrease of knee joint stiffness during landing after fatigue can help reduce the risk of ACL injury to a certain extent, which can also be regarded as a protection mechanism of the human body itself from the impact of landing. However, when the fatigue deepens, the neuromuscular control ability is further weakened, resulting in weakened absorption of the impact force in the lower limbs, which will increase the passive load of the lower limb bones and soft tissues. In the initial stage of landing, the knee and ankle joints of the lower limbs passively produce a flexion moment under the influence of the impact force, and in order to reduce the impact of the impact force on the lower limb musculoskeletal system, the human body passively produces an extension moment through the centrifugal contraction of the extensor muscles of the lower limbs. Studies have estimated that the moments exerted by the knee flexor muscle groups account for 10.5% to 16.8% of the synthesized joint moments, which is much smaller than the moments generated by the knee extensors. Fatigue of the knee extensors resulted in participants having to adjust the landing cushion for a number of kinematic and kinetic variables, including a reduction in the amount of joint angle change at the knee, a reduction in peak knee and hip angular velocity, and an increase in knee stiffness.

III. C. 3) Ground reaction forces and rigidity

Repetitive, passive landing impacts in sport have long been recognized as a major cause of overuse injuries to the lower extremities, which produce a combined fatigue effect and inhibit skeletal muscle remodeling and repair processes. According to this mechanism, the key factor contributing to overuse resulting in sports injuries is fatigue, and the repetitive, long distance of sports is one of the potential factors that may cause fatigue. In this study, during the fatigue intervention, there was no significant difference in ground reaction forces such as the first peak value, the second peak value, and the average and maximum loading rates before and after fatigue, which is consistent with the findings of related researchers. In addition, there was no statistically significant difference in the ground reaction forces before and after the fatigue intervention. Meanwhile, no significant differences were found in the braking force and propulsive force in the horizontal direction during the fatigue process, which is consistent with previous studies. Therefore, both before and after fatigue and throughout the fatigue process indicate that fatigue is not linearly correlated with impact force and that the magnitude of impact force does not change significantly as fatigue develops and occurs. In addition, load factor, defined as the amount of change in vertical ground reaction force per unit time, is often used as a sensitive and important indicator of impact force in running and jumping sports in the field of biomechanics, and the magnitude of load factor is more reflective of the relationship between running impacts and running injuries than the peak impact value. However, in the present study, there was no significant difference between the mean and maximum loading rates throughout the fatigue progression, which is the same as the results of previous studies, indicating that fatigue factors do not have a statistically significant effect on loading rates while maintaining the current sports posture. In addition, neuromuscular fatigue induced by prolonged physical activity leads to decreased control, and as the ability of the neuromusculoskeletal system to cushion impacts decreases, the chances of lower extremity injury increase. □□

In summary, from the present study, there was no statistical difference in fatigue to landing impact and loading rates during sports fatigue, which may be explained by the fact that impact and loading rates are closely related to the way of touching the ground. Without changing the sports posture, there is no linear relationship with lower limb muscle fatigue, and the human lower limb musculoskeletal system in prolonged sports, the lower limb three joints and their constituent muscles will take the initiative to adapt to and transfer and attenuate the impact of the grounding in order to reduce the impact injury, and to better ensure the effectiveness of sports teaching.

It has been suggested that if exercising at constant velocity until fatigue, vertical stiffness decreases with the fatigue process, and the change in vertical stiffness has an inverse relationship with the change in vertical displacement of the lower limb during the support period, while it is not related to vGRF. The findings of the present study validate these results, in that during the fatigue process of the sport, the vertical stiffness decreased significantly in both moderate and severe fatigue states compared to the pre-fatigue state, which corresponds to a significant increase in the amount of change in the vertical displacement of the center of gravity in both moderate and severe fatigue states. In contrast, at the lowest moment of the center of gravity, vGRF was not statistically different at the four moments, which can be explained by the increase in the center of gravity displacement causing a decrease in the vertical stiffness.

IV. Conclusion

Through the high-performance computational simulation analysis of this study, the changing rules of biomechanical characteristics under different fatigue states in sports and their effects on teaching effects were revealed. It was found that the biomechanical characteristics of lower limb joint kinematics, kinetic indexes and stiffness of athletes under fatigue state changed significantly. Specifically, the flexion angle of the hip joint decreased to 36.78±9.48° and 40.12±10.54° in the moderate and severe fatigue state respectively, which was significantly reduced compared with the 43.19±7.38° in the non-fatigue state, and the flexion angle of the knee joint decreased from 20.75±9.72° in the non-fatigue state to 17.46±8.05° in the moderate fatigue state and 16.94±10.05° in the severe fatigue state respectively. The knee flexion angle also decreased from 20.75±9.72° in the no-fatigue state to 17.46±8.05° in the moderate fatigue state and to 16.94±10.24° in the severe fatigue state, respectively, the peak knee extension moment decreased from 2.76±0.15 N-m/kg in the no-fatigue state to 2.12±0.15 N-m/kg in the moderate fatigue state, and vertical stiffness decreased from 58.73±14.34 KN/m in the no-fatigue state to 50.26±9.61 KN/m in the moderate fatigue state. 50.26±9.61KN/m for moderate fatigue and 46.47±10.45KN/m for severe fatigue, at the same time, the vertical displacement of the center of gravity increased from 3.28±0.61cm for no fatigue to 3.98±0.76cm for severe fatigue, however, there was no significant difference between the ground reaction force parameters before and after fatigue, which indicated that fatigue was not linearly correlated with impact force. These changes in biomechanical characteristics reflect the self-protection mechanism of the human body in the fatigue state, which reduces the risk of sports injuries by changing the angle and stiffness of the lower limb joints. The results of the study have important guiding significance for physical education teaching, and it is suggested that the training load should be reasonably arranged in physical education teaching to avoid sports injury caused by overfatigue, and at the same time, the simulation model can be utilized to assist the teaching and to improve the students' understanding of the principles of sports biomechanics.

Funding

This work was supported by General Science and Technology Projects of Beijing Municipal Education Commission Award (ID: KM202410009005),

The University-Industry Collaborative Education Program of the Ministry of Education of China (ID: 241200676181521).

References

[1] Quennerstedt, M. (2019). Physical education and the art of teaching: Transformative learning and teaching in physical education and sports pedagogy. Sport, Education and Society.

[2] van Beijsterveldt, A. M., Richardson, A., Clarsen, B., & Stubbe, J. (2017). Sports injuries and illnesses in first-year physical education teacher education students. BMJ open sport & exercise medicine, 3(1).

[3] Li, J., & Wang, L. (2022). Study on the evaluation of exercise effect in physical education teaching under the application of random forest model. Mobile Information Systems, 2022(1), 7220064.

[4] Barendrecht, M., Barten, C. C., Van Mechelen, W., Verhagen, E., & Smits-Engelsman, B. C. (2023). Injuries in physical education teacher students: Differences between sex, curriculum year, setting, and sports. Translational sports medicine, 2023(1), 8643402.

[5] Bessa, C., Hastie, P., Ramos, A., & Mesquita, I. (2021). What actually differs between traditional teaching and sport education in students' learning outcomes? A critical systematic review. Journal of sports science & medicine, 20(1), 110.

[6] Teferi, G., & Endalew, D. (2020). Methods of Biomechanical Performance Analyses in Sport: Systematic Review. American Journal of Sports Science and Medicine, 8(2), 47-52.

[7] Bourantanis, A., Nomikos, N., & Wang, W. (2024). Biomechanical Insights in Ancient Greek Combat Sports: A Static Analysis of Selected Pottery Depictions. Sports, 12(12), 317.

[8] Firdiansyah, B. (2022, July). Biomechanics Analysis of Static Stretching using Dartfish Express in PGMI Sports Learning. In ICIE: International Conference on Islamic Education (Vol. 2, pp. 115-124).

[9] Alzahrani, A., & Ullah, A. (2024). Advanced biomechanical analytics: Wearable technologies for precision health monitoring in sports performance. Digital Health, 10, 20552076241256745.

[10] Hollander, K., Zech, A., Rahlf, A. L., Orendurff, M. S., Stebbins, J., & Heidt, C. (2019). The relationship between static and dynamic foot posture and running biomechanics: A systematic review and meta-analysis. Gait & posture, 72, 109-122.

[11] Song, Y., Zhao, X. X., Finnie, K. P., & Shao, S. R. (2018). Biomechanical analysis of vertical jump performance in well-trained young group before and after passive static stretching of knee flexors muscles. Journal of Biomimetics, Biomaterials and Biomedical Engineering, 36, 24-33.

[12] Bezodis, N. E., Willwacher, S., & Salo, A. I. T. (2019). The biomechanics of the track and field sprint start: a narrative review. Sports medicine, 49(9), 1345-1364.

[13] Wang, H., Chen, C., He, Y., Sun, S., Li, L., Xu, Y., & Yang, B. (2024). Easy Rocap: A Low-Cost and Easy-to-Use Motion Capture System for Drones. Drones, 8(4), 137.

[14] Valevicius, A. M., Jun, P. Y., Hebert, J. S., & Vette, A. H. (2018). Use of optical motion capture for the analysis of normative upper body kinematics during functional upper limb tasks: A systematic review. Journal of electromyography and kinesiology, 40, 1-15.

[15] Annavini, E., & Boulland, J. L. (2023). Integrated software for multi-dimensional analysis of motion using tracking, electrophysiology, and sensor signals. Frontiers in Bioengineering and Biotechnology, 11, 1250102.

[16] Ma, Q., & Huo, P. (2022). Simulation analysis of sports training process optimisation based on motion biomechanical analysis. International Journal of Nanotechnology, 19(6-11), 999-1015.

[17] Balaprakash, P., Dongarra, J., Gamblin, T., Hall, M., Hollingsworth, J. K., Norris, B., & Vuduc, R. (2018). Autotuning in high-performance computing applications. Proceedings of the IEEE, 106(11), 2068-2083.

[18] Jagiella, N., Rickert, D., Theis, F. J., & Hasenauer, J. (2017). Parallelization and high-performance computing enables automated statistical inference of multi-scale models. Cell systems, 4(2), 194-206.

[19] Mustafa, A., & Hameed, N. (2023). Advanced Computing Techniques for Real-Time Data Processing and High-Performance Computing. Journal of Advanced Computing Systems, 3(8), 1-8.

[20] Schwartz, M., & Dixon, P. C. (2018). The effect of subject measurement error on joint kinematics in the conventional gait model: Insights from the open-source pyCGM tool using high performance computing methods. PloS one, 13(1), e0189984.

[21] Wang Yangang,Liu Yebin,Tong Xin,Dai Qionghai & Tan Ping. (2018). Outdoor Markerless Motion Capture with Sparse Handheld Video Cameras .IEEE transactions on visualization and computer graphics,24(5),1856-1866.

[22] Adam Rauff,Michael R Herron,Steve A Maas & Jeffrey A Weiss. (2024). An Algorithmic and Software Framework to Incorporate Orientation Distribution Functions in Finite Element Simulations for Biomechanics and Biophysics. Acta biomaterialia,192,151-164.

[23] Abdul Aziz Vaqar Hulleck,Muhammed Abdullah,Farah Hamed,Rateb Katmah,Kinda Khalaf & Marwan El Rich. (2024). Ground Reaction Forces and Moments in Stroke Survivors: Experimental versus AnyBody Model Predictions. Annual International Conference of the IEEE Engineering in Medicine and Biology Society. IEEE Engineering in Medicine and Biology Society. Annual International Conference,2024,1-5.

[24] Zhu Yancong,Li Haojie,Lyu Shaojun,Shan Xinying,Jan YihKuen & Ma Fengling. (2023). Stair-climbing wheelchair proven to maintain user's body stability based on AnyBody musculoskeletal model and finite element analysis. PloS one,18(1),e0279478-e0279478.